PHYSICAL REVIEW C, VOLUME 64, 041302(R)

Investigation of antimagnetic rotation in ^{100}Pd

S. Zhu, U. Garg, A. V. Afanasjev, S. Frauendorf, and B. Kharraja
Department of Physics, University of Notre Dame, Notre Dame, Indiana 46556

S. S. Ghugre and S. N. Chintalapudi
IUCDAEF-Calcutta Centre, Sector III/LB-8, Bidhan Nagar, Calcutta 700 064, India

R. V. F. Janssens, M. P. Carpenter, F. G. Kondev, and T. Lauritsen
Physics Division, Argonne National Laboratory, Argonne, Illinois 60439

(Received 13 March 2001; published 11 September 2001)

High spin states have been studied in the nucleus ^{100}Pd with the aim of investigating the novel phenomenon of ''antimagnetic rotation.'' A cascade of four ''rotational-band-like'' transitions is proposed as corresponding to antimagnetic rotation, based on the observed spectroscopic properties and a comparison with calculations in the configuration-dependent cranked Nilsson-Strutinsky formalism.

DOI: 10.1103/PhysRevC.64.041302 PACS number(s): 27.60.+j, 23.20.Lv, 21.10.Tg, 21.60.Ev

''Magnetic rotation'' has been a topic of great interest and activity in nuclear structure in the past few years. Strong $M1$ bands have been observed in the nuclei of the Pb and Sn regions. These bands, while as regularly spaced as the bands observed in well-deformed and even superdeformed nuclei, show very weak $E2$ transitions, implying a small deformation [1–3]. Lifetime measurements confirmed that the deformations are of the order of $\varepsilon_2 \sim 0.1$, in contrast to the time-honored concept that only well-deformed nuclei develop rotational bands [4,5]. The explanation of this apparent contradiction was given in terms of the ''shears mechanism'' [6,7]. The regular level spacing of the $M1$ bands indicates that there must be a rotational degree of freedom. In case of the Pb nuclei, a pair of $h_{9/2}$, $i_{13/2}$ protons and between one and three $i_{13/2}$ neutron holes generate the angular momentum. The particles are in stretched coupling and so are the holes. Their angular momenta form the two ''blades'' of a pair of shears, which gradually close as the total angular momentum increases along the band. The particles and holes move in circular orbitals in the planes perpendicular to their angular momenta. These loops of nucleonic currents are crossed when the shears are open. This anisotropic arrangement breaks the rotational symmetry. ''Magnetic rotation'' alludes to these currents and the magnetic moment they create, generating the strong $M1$ radiation.

Definitive tests of this interpretation have come from the behavior of the $B(M1)$ transition probabilities as a function of spin. As predicted, the $B(M1)$ values in these bands drop in a characteristic manner with increasing spin [4,5,8]. The interaction between the loops, which determines the moment of inertia, is due to a slight quadrupole polarization of the nucleus. Calculations based on the tilted axis cranking (TAC) model [6] confirmed this interpretation in a quantitative way [4,5,9]. A more phenomenological treatment of the shears mechanism has been put forward by Macchiavelli *et al.* [10] who ascribe the interaction between the loops to the exchange of quadrupole phonons. Their prescription provides a consistent picture for the observed energies, and the $B(M1)$ and $B(E2)$ values, and utilizes a few parameters such as the particle-phonon coupling strength, and the effective charges and g factors.

Associated with, and complementary to, magnetic rotation is the concept of ''antimagnetic rotation'' [11,7]. In this scenario, the coupling for the $A \sim 110$ case is such that two pairs of stretched $\pi g_{9/2}$ holes point in opposite directions and gradually align along the direction of the stretched $h_{11/2}$ neutrons (creating a ''fork,'' with the neutrons forming the middle prong and the proton holes forming two symmetric side prongs; see Fig. 1). Clearly, such an arrangement also breaks the rotational symmetry with respect to the vector $\vec{I}$ of the total angular momentum and, thus, leads to a rotational band. Angular momentum, then, is generated mainly by ''bending'' the side prongs. In contrast to the $M1$ bands, this arrangement is symmetric with respect to a rotation about $\vec{I}$ by an angle of π. Consequently, the signature, α, is a good quantum number and the resulting ''fork bands'' have a regular $\Delta I = 2$ structure, in contrast with the $\Delta I = 1$ sequences associated with the ''shears bands.'' The magnetic moment disappears in the symmetric arrangement of the current loops, which nevertheless specify the orientation. (The term ''antimagnetic'' rotation alludes to the analogy with ferro and antiferromagnetism.) The experimental signature of ''antimagnetic'' rotation, thus, is very small deformation ($\varepsilon_2 \leqslant 0.15$) and, at the same time, a regular cascade of $E2$ transitions. This is a novel phenomenon, because in conventional wisdom regular bands appear only if there is enough deformation for collective angular momentum.

A most appropriate place to look for these ''fork bands'' is in the $Z < 50$ and $N > 50$ region. To create ''side prongs'' that are sufficiently long, one would have to have two pairs of $g_{9/2}$ proton holes. For the ''middle prong,'' one would require one (or more) $h_{11/2}$ neutrons. At the same time, the final configuration must be associated with a small deformation. This restricts the choice, basically, to $N = 50$–55: having ''too many'' neutrons beyond $N = 50$ would lead to deformations larger than suitable for magnetic rotation (in general,

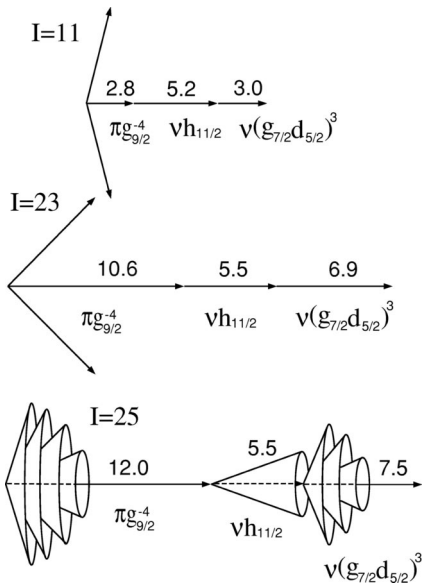

FIG. 1. The composition of the total angular momentum within the configuration [4,1] given at different spin values (see text). The calculations were performed along the deformation path of this configuration. The individual contributions of valence particles and holes are shown only in the bottom panel, where the precession of angular momenta around the axis of rotation (which at termination coincides with the symmetry axis) is illustrated. In the upper two panels, the contribution of the two pairs of the $\pi g_{9/2}$ holes and all active $\nu(g_{7/2},d_{5/2})$ particles is shown without specification of the contribution of each particle (hole).

''collective rotation'' appears to set in rapidly beyond $N=54$ in this region [12]), while being too close to $N=50$ would not readily bring about the $h_{11/2}$ neutrons into the picture.

Based on these considerations, the nucleus ^{100}Pd($Z=46$, $N=54$) is expected to be among the nuclei most likely to exhibit antimagnetic rotational behavior. In this Rapid Communication, we present results of an investigation of ''antimagnetic'' rotation in this nucleus.

High-spin states in ^{100}Pd were populated following the ^{72}Ge(^{35}Cl, $\alpha p2n$)^{100}Pd reaction at a bombarding energy of 135 MeV. The experiment was carried out at the ATLAS facility at Argonne National Laboratory and the Gammasphere detector array was employed in its ''stand alone'' mode. A ^{72}Ge target (of 1 mg cm^{-2} thickness) was evaporated onto a 15 mg cm^{-2} thick gold foil. A thin (40 μg cm^{-2}) Al layer was evaporated between the target and the backing to avoid migration of target material into gold. At the time of the experiment, the Gammasphere spectrometer consisted of 101 Compton-suppressed Ge detectors. The trigger level for the device was set to accept a minimum of three Compton-suppressed Ge detectors in prompt coincidence. The total data set consisted of approximately 2×10^9 ''triple coincidence'' events.

The level scheme for ^{100}Pd obtained from this experiment is shown in Fig. 2. It has been constructed using standard analysis procedures; the RADWARE analysis package [13] was employed. The selectivity afforded by ''double gating'' and the presence of many crossover transitions in the level scheme provide many checks of the placement and ordering of transitions, and serve to bolster confidence in the correctness of the proposed level scheme. The same holds true for the multipolarity assignments which are based primarily on the analysis of the so-called DCO ratios. In our procedure, coincidence gates are placed on spectra from the forward-angle (32° and 37°) detectors, and the γ rays measured at 90° and at backward angles (143° and 147°) are sorted along the two axes of the matrices. The ratios, $R=I_\gamma$(backward)/I_γ(90°), can be used to make reliable spin assignments by comparing the ratios of the new γ lines with those of previously-known γ rays whose multipolarity is already firmly established. Supporting evidence for the spin assignments is provided, in many cases, by the presence of crossover transitions. The averaged value of R is 1.0(3) for known $E2$ transitions in ^{100}Pd and 0.5(1) for the known dipole transitions.

The level scheme has overall good agreement with the most recent high-spin work [14], but has been significantly expanded. The level sequence of interest from the point of view of antimagnetic rotation is in the negative-parity cascade and consists of transitions of 1071-, 1388-, 1582-, and 1752-keV (marked ''B1'' in Fig. 2). A coincidence spectrum showing these and other ''nearby'' transitions is presented in Fig. 3. This sequence exhibits the regular increase in transition energy with spin which is characteristic of a rotational band. The moments of inertia, $\mathcal{J}^{(1)}$ and $\mathcal{J}^{(2)}$, associated with this sequence show a smooth behavior expected of ''regular'' rotational bands (see inset, Fig. 2). In addition, the DCO ratios for these transitions are consistent with an $E2$ multipolarity—the values for the ratio, R, are 0.9(2), 0.8(1), 0.7(3), and 1.0(5), respectively, for the 1071-, 1388-, 1582-, and 1752-keV transitions. However, as described later, the lifetimes of these transitions correspond to very small deformations associated with the underlying structure. Also, although this sequence of $E2$ transitions begins with the 809-keV ($11^-\rightarrow9^-$) transition, the ''rotational-band-like'' properties expected for antimagnetic rotation appear only at higher spins (after the band crossing; see discussion below).

In order to understand the features of this structure, calculations have been performed using the configuration-dependent cranked Nilsson-Strutinsky formalism. These calculations are analogous to those performed for other nuclei in the $A\sim100$ region (see Refs. [15–17] for details). In this formalism, the configurations are determined by the number of particles in the N shells of the rotating basis [16,18]. The energy of each configuration at each spin is minimized in the deformation space ($\varepsilon_2,\varepsilon_4,\gamma$) which allows the development of the shape within specific configurations to be traced as a function of spin. The pairing correlations are neglected in the calculations. Since the single-particle parameters are not very well known in the $A\sim100$ region, standard Nilsson potential parameters of Ref. [18] have been employed.

The results of the calculations are presented in Fig. 4 and compared with experimental data. The calculations indicate that the configuration [4,1] terminating at $I=25\hbar$ can be assigned at high spin to the observed band B1, thus suggesting that this band has been seen up to termination. The level of agreement between experiment and theory is similar to the

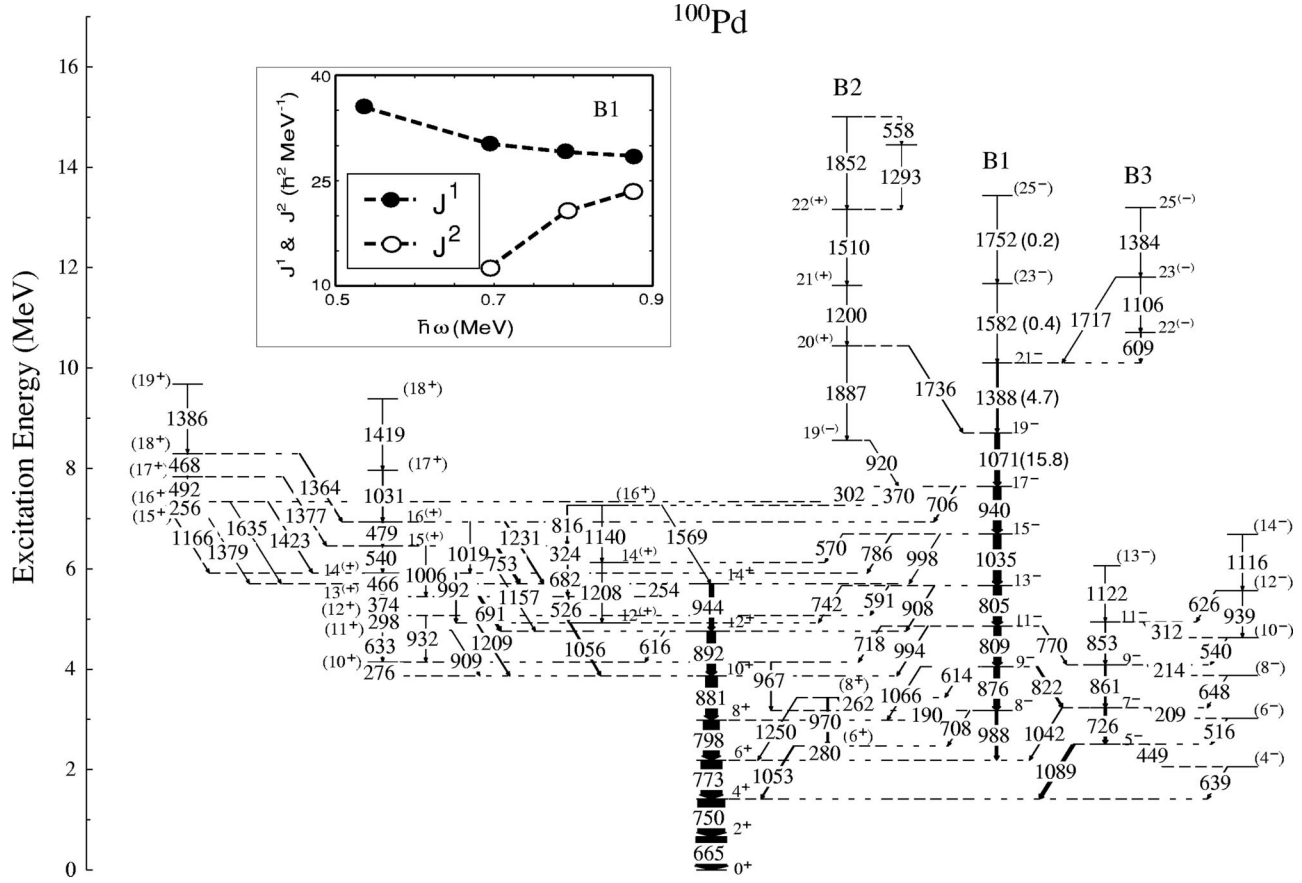

FIG. 2. Level scheme of ^{100}Pd obtained in this work. The widths of the arrows are proportional to the relative intensities of the transitions. For the transitions proposed as corresponding to antimagnetic rotation (AMR), intensities relative to the 665-keV line are given in parentheses next to the transition energies. In general, the uncertainties in transition energies are ~0.5 keV and in the intensities ~10%. The moments of inertia, $\mathcal{J}^{(1)}$ and $\mathcal{J}^{(2)}$, for the AMR transitions are shown in the inset.

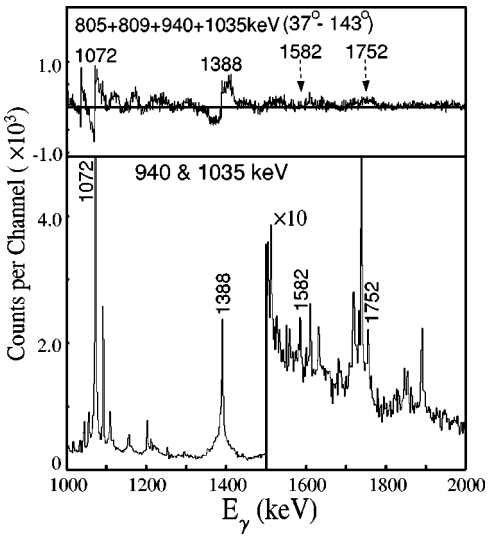

FIG. 3. The lower panel shows double-gated coincidence spectrum for the transitions in band B1. The upper panel shows the experimental ''difference spectrum'' (see text) obtained by summing a number of single gates; the coincidence gates are indicated in both cases.

one seen for terminating bands in neighboring nuclei (see Sec. 7.5 of Ref. [16] for details). The experimental ($E - E_{RLD}$) curve for band B1 (see the bottom panel of Fig. 4), where $E_{RLD}=0.015I(I+1)$ is the standard rotational reference, shows the band crossing at $I=15\hbar$. This crossing might be due to either a paired band crossing or an unpaired band crossing between the [4,1] and [3(1),0] configurations. Due to uncertain spin-parity assignments of the side structures ''B2'' and ''B3,'' no attempt was made to assign configurations to them.

Under this configuration assignment, the angular momentum in band B1 is built by gradual alignment of two pairs of proton $g_{9/2}$ holes, one $h_{11/2}$ neutron, and three ($g_{7/2}$,$d_{5/2}$) neutrons along the axis of rotation. Figure 1 illustrates how the angular momentum is built from the contributions of valence particles and holes. Already at spin $I=11\hbar$, the $h_{11/2}$ neutron is almost completely aligned along the axis of rotation and higher spin states are predominantly built by alignment of proton $g_{9/2}$ holes. This is consistent with antimagnetic rotation which is mainly generated by ''bending'' the side prongs, formed by pairs of stretched $\pi g_{9/2}$ holes along the axis of rotation. These holes account for almost half of the angular momentum available in the configuration. This is

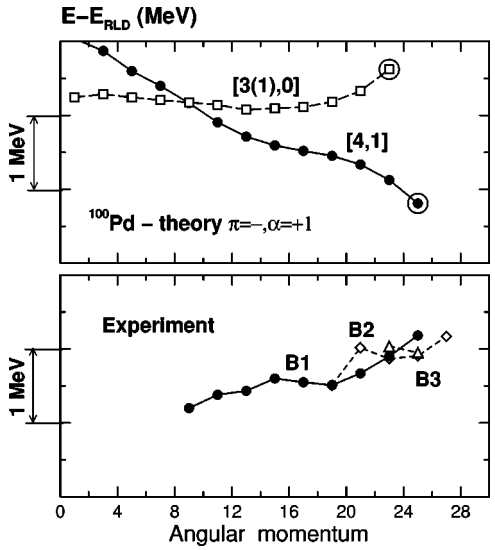

FIG. 4. Excitation energy relative to an $I(I+1)$ rigid rotor reference as a function of I for the experimental (bottom) and calculated (top) bands with $\pi=-,\alpha=+1$. The shorthand notation $[p_1(p_2),n]$, where p_1 is the number of proton holes in $g_{9/2}$ orbitals, p_2 is the number of proton holes in the $N=3$ orbitals, and n is the number of neutrons in $h_{11/2}$ orbitals relative to a spherical ^{100}Sn core, is used for configuration labeling. For configurations with no proton holes in the $N=3$ orbitals, p_2 is omitted. The detailed structure of the [4,1] and [3(1),0] configurations is $\pi(g_{9/2})^{-4}_{12}\otimes\nu(h_{11/2})^{1}_{11/2}(g_{7/2}\,d_{5/2})^{3}_{15/2}$ and $\pi(g_{9/2})^{-3}_{21/2}(N=3)^{-1}_{5/2}\otimes\nu(g_{7/2}\,d_{5/2})^{4}_{10}$, respectively. In these structures, the subscripts show the aligned spin at termination. Calculated terminating states are encircled.

larger than in the case of the proposed antimagnetic band in ^{109}Cd [19], where such contribution accounts only for approximately one-fourth of the available angular momentum, suggesting that the structure observed here is a better example of antimagnetic rotation.

An important consideration in identifying this structure with antimagnetic rotation is the size of the $B(E2)$ transition probabilities. Unfortunately, because of the limited statistics for the lines of interest in the present experiment (these lines are only a few percent of the intensity in the ^{100}Pd channel, which itself represents less than 10% of the total reaction cross section), a full DSAM analysis was not feasible. Nevertheless, one can discern the presence of combined lifetimes (state + sidefeeding) comparable to the stopping times of the recoiling ^{100}Pd nuclei in the target + backing ($\sim$1.2 ps) for these γ rays. This is indicated by a characteristic ''oscillatory pattern'' in the ''difference spectrum'' (obtained by subtracting the gated spectrum from the backward detectors from that corresponding to the forward detectors).[1] One such ''difference spectrum'' is shown in the upper panel of Fig. 3. The

[1] γ rays emitted from partially slowed recoils will show a typical Doppler-shifted line shape with a peak at the unshifted energy and a high- or low-energy tail depending on the angle of detection. The forward-backward subtraction, then, results in an oscillatory pattern with a width equal to twice the full Doppler shift [20].

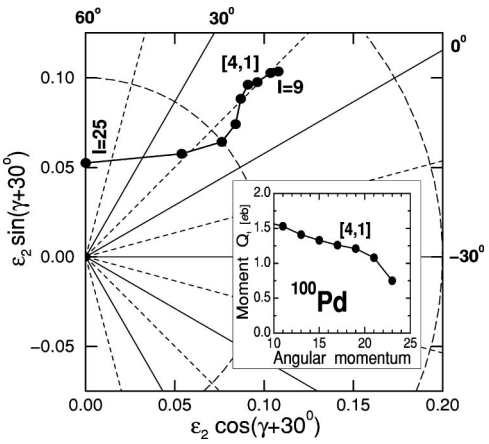

FIG. 5. Shape trajectory in the (ε_2,γ) plane for the [4,1] configuration. The deformation points are given in steps of $2\hbar$ starting from the state with $I=9\hbar$. The corresponding transition quadrupole moments Q_t (e b) calculated according to Eqs. (67),(68) of Ref. [16] are shown in the inset.

observed ''oscillatory pattern'' is quite clear for the 1071- and 1382-keV γ rays. (It is difficult to say anything about the 1582- and 1752-keV transitions because of the rather poor statistics for these transitions in the angle-sorted spectra.) The combined lifetimes of the transitions of interest are, thus, consistent with a small associated deformation (any significant deformation would result in much shorter lifetimes than those indicated by the present data; for example, for an associated deformation of $\varepsilon_2=0.2$, the 1071-keV transition would have $\tau\sim0.3$ ps).

The calculated shape trajectory in the (ε_2,γ) plane as a function of spin for the [4,1] configuration and the associated transition quadrupole moments Q_t (e b) are shown in Fig. 5. The $B(E2)$ values for the transitions of interest are 7.6–21.4 Weisskopf units and the associated lifetimes range between $\sim$0.3 ps and $\sim$1.0 ps. These lifetimes are in agreement with experimental estimates discussed above. Combined with the experimental moments of inertia $\mathcal{J}^{(2)}$ extracted for the transitions of interest, one obtains $\mathcal{J}^{(2)}/B(E2)$ ratios in the range of 230–1120 $\hbar^2\mathrm{MeV}^{-1}(e\,\mathrm{b})^{-2}$. The typical ratio for a well-deformed collective rotor would be $\sim10\hbar^2\mathrm{MeV}^{-1}(e\,\mathrm{b})^{-2}$, i.e., more than an order of magnitude smaller. This implies that the nucleus ^{100}Pd exhibits a rotational sequence although it is nearly spherical and, as argued earlier, this sequence provides a good case for antimagnetic rotation. Indeed, this value is comparable to that obtained for the purest magnetic rotor, ^{106}Cd [21]. In comparison, this ratio for ^{109}Cd is $\sim165\hbar^2\mathrm{MeV}^{-1}(e\,\mathrm{b})^{-2}$ [19].

Evidence for antimagnetic rotation in ^{100}Pd is, thus, provided by (a) the observation of a ''rotational-band-like'' cascade of transitions in which the angular momentum is mainly ($\approx$50%) generated by ''bending'' the side prongs, formed by the pairs of stretched $\pi g_{9/2}$ holes, along the axis of rotation; (b) the small deformation associated with these transitions, as evidenced by the limited lifetime information available from this experiment, and in agreement with expectations from theoretical results; and, (c) very large

estimated $\mathcal{J}^{(2)}/B(E2)$ ratios (in the range of 230–1120 $\hbar^2\mathrm{MeV}^{-1}(e\,\mathrm{b})^{-2}$). Clearly a full DSAM measurement of lifetimes of the lines of interest would be most desirable. Still, the combination of factors enumerated above provides good evidence for this very interesting and novel phenomenon.

While this manuscript was being finalized, the authors became aware of a very recent report on ^{100}Pd by Perez *et al.* [22]. The level scheme presented in Fig. 2 is in very good overall agreement with that presented therein. However, the central issue of antimagnetic rotation has not been addressed in Ref. [22].

This work was supported in part by the National Science Foundation (Grant No. PHY99-01133), the U.S. Department of Energy, Nuclear Physics Division, under Contract No. W31-109-ENG-38, and the University Grants Commission, Government of India.

[1] G. Baldsiefen *et al.*, Z. Phys. A **343**, 245 (1992).
[2] R.M. Clark *et al.*, Z. Phys. A **342**, 371 (1992).
[3] A. Kuhnert *et al.*, Phys. Rev. C **46**, 133 (1992).
[4] R.M. Clark *et al.*, Phys. Rev. Lett. **78**, 1868 (1997).
[5] N.S. Kelsall *et al.*, Phys. Rev. C **61**, 011301(R) (1999).
[6] S. Frauendorf, Nucl. Phys. **A557**, 259c (1993).
[7] S. Frauendorf, Rev. Mod. Phys. **73**, 463 (2001).
[8] E.F. Moore *et al.*, Phys. Rev. C **51**, 115 (1995).
[9] G. Baldsiefen *et al.*, Nucl. Phys. **A574**, 521 (1994).
[10] A.O. Macchiavelli *et al.*, Phys. Rev. C **57**, R1073 (1998).
[11] S. Frauendorf, Z. Phys. A **358**, 163 (1997).
[12] See, for example, J. Gizon *et al.*, Z. Phys. A **345**, 335 (1993).
[13] D.C. Radford, Nucl. Instrum. Methods Phys. Res. A **361**, 297 (1995).
[14] S. Tandel, S.B. Patel, Pragya Das, R.P. Singh, and R.K. Bhowmik, Z. Phys. A **357**, 3 (1997).
[15] I. Ragnarsson, A.V. Afanasjev, and J. Gizon, Z. Phys. A **355**, 383 (1996).
[16] A.V. Afanasjev, D.B. Fossan, G.J. Lane, and I. Ragnarsson, Phys. Rep. **322**, 1 (1999).
[17] J. Gizon *et al.*, Phys. Lett. B **410**, 95 (1997).
[18] T. Bengtsson and I. Ragnarsson, Nucl. Phys. **A436**, 14 (1985).
[19] C.J. Chiara *et al.*, Phys. Rev. C **61**, 034318 (2000).
[20] A description of this procedure, as well as some examples, is provided in M.W. Drigert *et al.*, Nucl. Phys. **A515**, 466 (1990).
[21] D.J. Jenkins *et al.*, Phys. Rev. Lett. **83**, 500 (1999).
[22] G.E. Perez *et al.*, Nucl. Phys. **A686**, 41 (2001).